Acta Crystallographica Section D
Biological Crystallography
ISSN 0907-4449

Preparation and crystallization of the stimulatory and inhibitory complexes of GTP cyclohydrolase I and its feedback regulatory protein GFRP

Nobuo Maita,[a] Kengo Okada,[a] Shoko Hirotsu,[a] Kazuyuki Hatakeyama[b] and Toshio Hakoshima[a]*

[a]Department of Molecular Biology, Nara Institute of Science and Technology, 8916-5 Takayama, Ikoma, Nara 630-0101, Japan, and [b]Department of Surgery, University of Pittsburgh, Pittsburgh, Pennsylvania 15261, USA

Correspondence e-mail: hakosima@bs.aist-nara.ac.jp

Received 11 December 2000
Accepted 30 May 2001

Mammalian GTP cyclohydrolase I is a decameric enzyme in the first and rate-limiting step in the biosynthesis of tetrahydrobiopterin, which is an essential cofactor for enzymes producing neurotransmitters such as catecholamines and for nitric oxide synthases. The enzyme is dually regulated by its feedback regulatory protein GFRP in the presence of its stimulatory effector phenylalanine and its inhibitory effector biopterin. Here, both the stimulatory and inhibitory complexes of rat GTP cyclohydrolase I bound to GFRP were crystallized by vapour diffusion. Diffraction data sets at resolutions of 3.0 and 2.64 Å were collected for the stimulatory and inhibitory complexes, respectively. Each complex consists of two GTPCHI pentamer rings and two GFRP pentamer rings, with pseudo-52 point-group symmetry.

1. Introduction

In mammals, GTP cyclohydrolase I (GTPCHI; E.C. 3.5.4.16) is the first and rate-limiting enzyme in the biosynthesis of 6*R*-L-*erythro*-5,6,7,8-tetrahydrobiopterin (BH_4) from GTP (Nichol *et al.*, 1985). BH_4 is an essential cofactor for nitric oxide synthase (NOS) (Tayeh & Marletta, 1989) and also for three enzymes: phenylalanine hydroxylase, tyrosine hydroxylase and tryptophan hydroxylase (Nichol *et al.*, 1985). Interestingly, these enzymes participate in the production of neurotransmitters. Tyrosine hydroxylase converts tyrosine to L-DOPA, which is a precursor of dopamine and several catecholamines. Moreover, tryptophan hydroxylase converts tryptophan to a precursor of serotonin. Therefore, disorder of the BH4 level caused by GTPCHI mutations leads to disorders of neurotransmission. Innumerable medical studies describe relationships between disorder of the BH4 level and neurological diseases such as DOPA-responsive dystonia (DRD; Ichinose *et al.*, 1994) and malignant hyperphenylalaninemia (Ichinose *et al.*, 1995). Indeed, many mutations in the GTPCHI gene of DRD patients have been reported (Brique *et al.*, 1999). Moreover, a low level of BH_4 in cerebrospinal fluid has been found in Parkinsonian patients (Lovenberg *et al.*, 1979; Fujishiro *et al.*, 1990).

Mammalian GTPCHIs have been shown to exhibit a unique form of allosteric regulation by interacting with the GTPCHI feedback regulatory protein (GFRP) in the presence of phenylalanine or biopterin (Harada *et al.*, 1993; Milstien *et al.*, 1996). GTPCHI and GFRP can form a stimulatory complex in the presence of >200 m*M* L-phenylalanine, which is the substrate of phenylalanine hydroxylase (Yoneyama & Hatakeyama, 1998). Recent studies using gel filtration (Yoneyama *et al.*, 1997; Yoneyama & Hatakeyama, 1998) suggest that free GFRP forms a pentamer and that two GFRP pentamers bind the GTPCHI decamer, thereby assembling a stimulatory $(GTPCHI)_{10}$–$2(GFRP)_5$ complex. Similarly, GTPCHI and GFRP form a BH_4-induced inhibitory $(GTPCHI)_{10}$–$2(GFRP)_5$ complex in the presence of the substrate GTP or its non-productive substrate analogue dGTP (Yoneyama & Hatakeyama, 1998). In the absence of these effectors, GFRP is unable to bind GTPCHI. To understand the mechanisms by which GFRP regulates GTPCHI, we have crystallized the stimulatory and inhibitory complexes. The monomeric GTPCHI and GFRP have molecular masses of about 25.7 kDa (230 residues) and 10.0 kDa (83 residues), respectively.

2. Materials and methods

Expression in *Escherichia coli* and purification of recombinant rat GTPCHI and GFRP were carried out following the methods previously described (Yoneyama *et al.*, 1997). Purified GTPCHI was concentrated to 6 mg ml^{-1} in 50 m*M* Tris–HCl buffer pH 7.5 containing 100 m*M* KCl, 1 m*M* EDTA and 1 m*M* DTT; purified GFRP was concentrated to 5 mg ml^{-1} in 50 m*M* MES–Na buffer pH 6.0. Both protein samples were stored at 193 K until the crystallization study.

To form the stimulatory complex, GTPCHI and GFRP were mixed in a buffer solution containing 50 m*M* Tris–HCl pH 7.5, 1 m*M* L-phenylalanine, 100 m*M* KCl, 1 m*M* EDTA and 1 m*M* DTT at final concentrations of 15 µ*M* GTPCHI and 15 µ*M* GFRP. The mixture was incubated at room temperature for 20 min and was then concentrated to 15 mg ml^{-1} by ultrafiltration using a 100 kDa cutoff Microcon (Amicon, USA). The sample solution was stored at 193 K.

To prepare the inhibitory complex, 6.4 ml of protein mixture (15 µ*M* GTPCHI, 15 µ*M* GFRP, 100 m*M* NaCl, 1 m*M* EDTA, 3 m*M* DTT, 0.3 m*M* dGTP, 45 µ*M* BH_2, 50 m*M* MES–Na pH 6) was incubated at room temperature for 20 min, followed by concentration to 10 mg ml^{-1}. We used BH_2 and dGTP instead of BH_4 and GTP because the former pair produce a more stable complex. The effects of these analogues on complex formation are of the same order as the native substrates BH_4 and GTP (Yoneyama & Hatakeyama, 1998).

Initial crystallization screening was carried out using the hanging-drop vapour-diffusion method using conventional crystallization screening solutions (Hampton Research, USA) at 288 K. The droplets were prepared by mixing 1 µl of protein solution with an equal volume of reservoir solution. The crystals obtained were dissolved and analyzed by 10%(*w*/*v*) sodium dodecyl sulfate–polyacrylamide gel electrophoresis (SDS–PAGE). Gels were stained with Coomassie brilliant blue. Crystals of the stimulatory complex were briefly transferred into a drop containing 35%(*v*/*v*) MPD, 100 m*M* Tris–HCl pH 7.5 and 5 m*M* L-phenylalanine, mounted in a rayon loop (Hampton Research) and then rapidly transferred into liquid nitrogen. These flash-frozen crystals were stored in liquid nitrogen until data collection. Crystallization screening of the inhibitory complex was performed using a vapour-diffusion technique in which 4 µl protein solution was mixed with 4 µl of precipitant solution on microbridges (Hampton Research, USA) equilibrated against 0.5 ml of reservoir solutions at 283 K. The single crystal obtained was mounted in a silicon-coated thin-wall glass capillary prior to data collection.

A native data set of the stimulatory complex was collected from one crystal at 100 K on beamline BL-6A of the Photon Factory (Tsukuba, Japan) using Fuji imaging plates (200 × 400 mm) by the rotation method with 2.0° oscillations. Diffraction data were processed with the programs *DENZO* and *SCALEPACK* (Otwinowski & Minor, 1997). Diffraction data of the inhibitory complex were collected on the beamline BL-18B at 293 K. Intensity data were collected on an ADSC Quantum CCD detector system. The crystal-to-detector distance was set to 180 mm. 150° of data were collected with an oscillation angle of 1°. The intensity data were indexed and scaled with the programs *DPS*/*MOSFLM* (Steller *et al.*, 1997; Leslie, 1992) and *SCALA* (Collaborative Computational Project, Number 4, 1994).

The self-rotation functions (Rossmann & Blow, 1962) were calculated using the program *POLARRFN* from the *CCP*4 package.

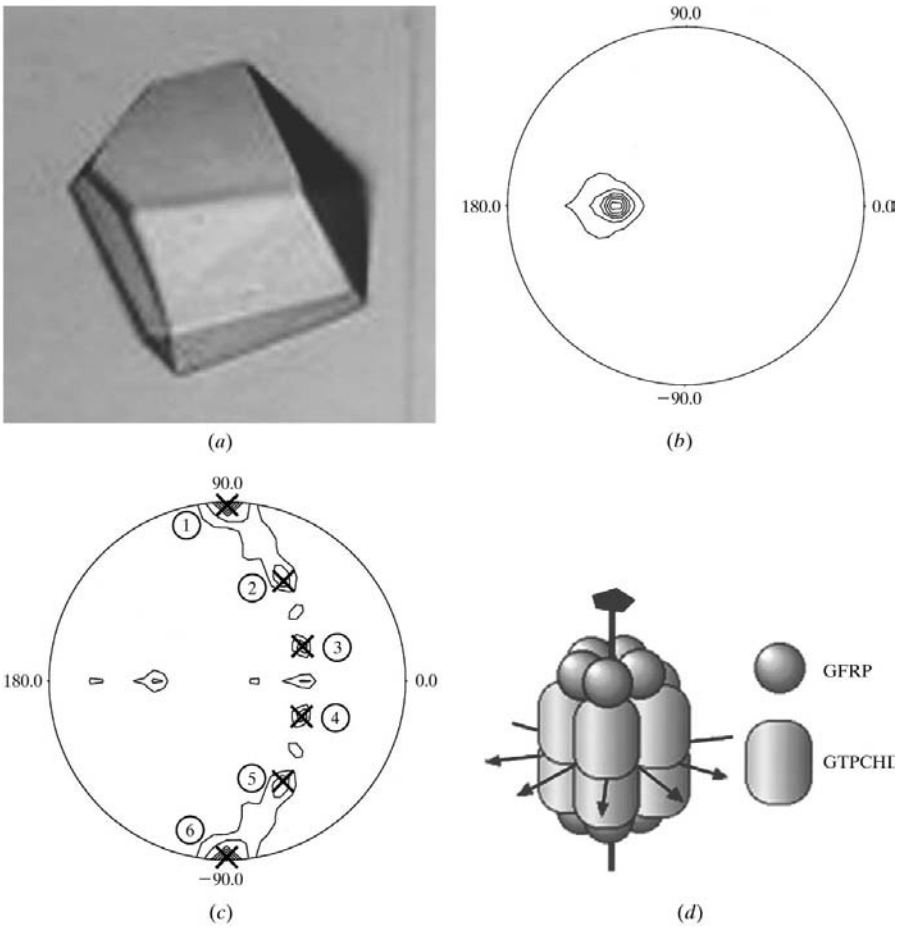

Figure 1
A typical crystal and the rotation functions of the stimulatory complex. (*a*) The monoclinic crystal of the stimulatory GTPCHI–GFRP–Phe complex (0.2 × 0.2 × 0.2 mm) in 35% MPD, 10 m*M* Phe pH 7.5. Self-rotation functions and the symmetry of the stimulatory complex. Stereographic projection of (*b*) the section $\kappa = 72°$ of the self-rotation function and (*c*) the section $\kappa = 180°$ of the self-rotation function of the stimulatory complex. The integration radius in the Patterson space is 35 Å and data are included from 15 to 5 Å. Contouring starts at the 2σ level and the interval is 1σ. The *c** axis is perpendicular to each projection, in which $\varphi = 0$, 90, 180 and $-90°$ are indicated with the *a* axis along $\varphi = 0°$. In (*b*), the peak at $\omega = 137.5$, $\varphi = 180°$ corresponds to the non-crystallographic fivefold axis. In (*b*), five peaks are marked by crosses with peak numbers; 1 ($\omega = 90.0$, $\varphi = 90.0°$), 2 (66.6, 63.0°), 3 (49.6, 24.9°), 4 (49.6, 335.1°), 5 (66.6, 297.0°) and 6 (90.0, 270.0°). These peaks are separated by 36° and correspond to the non-crystallographic twofold axes perpendicular to the fivefold axis. (*d*) Possible model of the stimulatory complex having 52 point-group symmetry. The fivefold axis (a thick line) and five twofold axes (thin lines) are indicated.

3. Results and discussion

Polygonal microcrystals of the stimulatory complex were first observed from droplets containing 65%(*v*/*v*) MPD solution pH 8. After refinement of the crystallization conditions, larger crystals were obtained from droplets consisting of 5 mg ml^{-1} protein solution containing 24%(*v*/*v*) MPD, 75 m*M* Tris–HCl pH 7.5 and 5 m*M* L-phenylalanine vapour-equilibrated against 0.5 ml reservoir solution [32%(*v*/*v*) MPD, 100 m*M* Tris–HCl pH 7.5, 5 m*M* L-phenylalanine] at 283 K. These crystals contained both GTPCHI and GFRP, as verified by SDS–PAGE. A single crystal (0.2 × 0.2 × 0.2 mm) used for X-ray data collection was grown in a week by the microseeding tech-

nique (Stura & Wilson, 1992) (Fig. 1*a*). The crystals were found to belong to the monoclinic space group $P2_1$, with unit-cell parameters a = 123.3 (2), b = 111.4 (3), c = 125.8 (3) Å, β = 97.69 (7)°. Assuming the presence of one complex in the asymmetric unit, the calculated value of the crystal volume per protein mass (V_M; Matthews, 1968) is 2.39 Å^3 Da^{-1}. This value corresponds to a solvent content of approximately 49%. The intensity data collection on the beamline BL-6A gave a set of intensity data at 3.0 Å resolution. The data-collection statistics are summarized in Table 1. Self-rotation function analyses of the data revealed a strong peak (51.6% height of the origin peak) representing a non-crystallographic fivefold axis (Fig. 1*b*) and also peaks representing five twofold axes perpendicular to the fivefold axis (Fig. 1*c*). A close inspection of the section κ = 180° of the self-rotation function revealed diffuse peaks between each pair of strong peaks. These peaks may suggest that five twofold axes of GFRP are shifted from those of GTPCHI by a rotation around the fivefold axis. These results indicate that the asymmetric unit contains decamers of GTPCHI and GFRP with pseudo-52 point-group symmetry. The C-terminal 120 residues of rat GTPCHI exhibit 66% sequence homology to the corresponding region of *E. coli* GTPCHI (221 residues). Recent crystallographic studies of *E. coli* GTPCHI have revealed a homodecameric complex characterized by docking of two pentameric rings having 52 point-group symmetry (Nar *et al.*, 1995). Together with this finding, our results of the self-rotation function analyses indicate that rat GTPCHI is likely to form a complex similar to that of *E. coli*. Moreover, in the present stimulatory complex, GFRP probably forms two pentameric rings that bind both sides of the GTPCHI pentameric rings (Fig. 1*d*). This conclusion is consistent with the proposed model from gel filtration (Yoneyama & Hatakeyama, 1998).

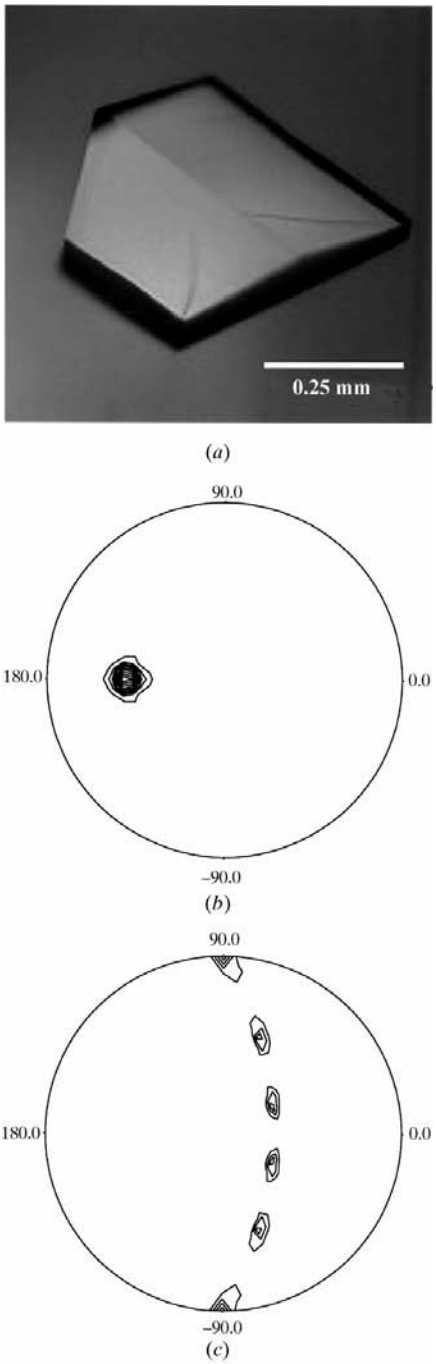

Figure 2
A typical crystal and the rotation functions of the inhibitory complex. (*a*) The typical crystal of the inhibitory GTPCHI–GFRP–BH2–dGTP complex. Self-rotation function map calculated from the diffraction data of the inhibitory complex. These maps were calculated in the resolution range 10–5 Å with a probe radius of 40 Å. The κ = 72° (*b*) and κ = 180° (*c*) section of the map are calculated with an integration radius of 40 Å using data in the resolution range 10–5 Å. Both maps are contoured at 1σ intervals from 3σ. The *c** axis is perpendicular to each projection with the *a* axis along φ = 0°.

Table 1
Data-collection statistics.

	Stimulatory	Inhibitory
X-ray source	PF BL-6A	PF BL-18B
Detector	Weissenberg camera	ADSC Quantum 4R
Temperature (K)	100	293
Wavelength (Å)	0.980	1.000
Distance (mm)	429.7	180.0
Oscillation angle (°)	2.0	1.0
Frames	102	150
Exposure time (s)	180	45
Resolution range (Å)	20–3.0	20–2.64
Space group	$P2_1$	$P2_1$
Unit-cell parameters		
a (Å)	123.3 (2)	122.3 (1)
b (Å)	111.4 (3)	111.8 (2)
c (Å)	125.8 (3)	130.6 (3)
β (°)	97.69 (7)	98.15 (3)
V_M (Å^3 Da^{-1})	2.39	2.33
V_{solv} (%)	49.0	47.2
Biochemical units	$(GTPCHI)_{10}$–$2(GFRP)_5$	$(GTPCHI)_{10}$–$2(GFRP)_5$
Observed reflections	334440	320560
Unique reflections	60700	102495
Mosaicity (°)	0.41	0.32
R_{sym}†‡ (%)	7.1 (25.9)	6.1 (39.3)
Completeness‡ (%)	89.9 (75.2)	99.2 (99.2)
Multiplicity	5.5	3.1
$I/\sigma(I)$‡	10.1 (2.8)	10.2 (1.8)

† $R_{sym} = \sum|I - \langle I\rangle|/\sum I$; calculated for all data. ‡ Values in parentheses are for the outer shell bins: 3.1–3.0 and 2.77–2.64 Å for the stimulatory and inhibitor complexes, respectively.

The crystals of the inhibitory complex were grown using 2-propanol and ammonium sulfate as precipitants. After refining the conditions, we found that large crystals appeared in drops containing 5 mg ml^{-1} protein and 50 m*M* MES–Na pH 6.0, 6%(*v*/*v*) 2-propanol, 0.1 *M* ammonium sulfate and 5 m*M* β-mercaptoethanol, vapour-equilibrated against a reservoir solution containing 100 m*M* MES–Na pH 6.0, 12%(*v*/*v*) 2-propanol, 0.2 *M* ammonium sulfate and 10 m*M* β-mercaptoethanol. Crystals grown under this optimized condition reached their maximum size within two weeks and had dimensions of 0.6 × 0.4 × 0.4 mm (Fig. 2*a*). The crystals were found to belong to space group $P2_1$, with unit-cell parameters a = 122.3 (1), b = 111.8 (2), c = 130.6 (3) Å, β = 98.15 (3)°. The diffraction data were collected to a resolution of 2.64 Å. The data set has a completeness of 99.2% in the outer shell and the redundancy of reflections was 3.1 with an overall R_{sym} of 6.1% (Table 1). Like the stimulatory complex, self-rotation functions indicate that the inhibitory complex also has pseudo-52 point-group symmetry (Figs. 2*b* and 2*c*). In the κ = 72° section, there is a peak of height 12σ at polar angles ω = 58.1, φ = 180, κ = 72°, corresponding to a fivefold axis. In the κ = 180° section of the map, five twofold axes are observed. Each neighbouring pair of these axes had an angle of nearly 36°. In addition, all these twofold axes were perpendicular to the fivefold axis.

For structure determination, heavy-atom derivatives and selenomethionine-substituted proteins are presently being prepared.

We would like to thank J. Tsukamoto for technical support in performing MALDI-TOF MS analysis. We also thank Dr T. Shimizu for his technical assistance with the data reduction. This work was supported by a grant from NIH of USA to KH (DK51257) and by a Grant-in-Aid for Scientific Research in Priority Areas B from the MESSC of Japan to TH (12147206). TH is a

member of the TARA Sakabe project of Tsukuba University.

References

Brique, S., Destaee, A., Lambert, J. C., Mouroux, V., Delacourte, A., Amouyel, P. & Chartier-Harlin, M. C. (1999). *NeuroReport*, **10**, 487–491.

Collaborative Computational Project, Number 4 (1994). *Acta Cryst.* D**50**, 760–763.

Fujishiro, K., Hagihara, M., Takahashi, A. & Nagatsu, T. (1990). *Biochem. Med. Metab. Biol.* **44**, 97–100.

Harada, T., Kagamiyama, H. & Hatakeyama, K. (1993). *Science*, **260**, 1507–1510.

Ichinose, H., Ohye, T., Matsuda, Y., Hori, T., Blau, N., Burlina, A., Rouse, B., Matalon, R., Fujita, K. & Nagatsu, T. (1995). *J. Biol. Chem.* **270**, 10062–10071.

Ichinose, H., Ohye, T., Takahashi, E., Seki, N., Hori, T., Segawa, M., Nomura, Y., Endo, K., Tanaka, H., Tsuji, S., Fujita, K. & Nagatsu, T. (1994). *Nature Genet.* **8**, 236–242.

Leslie, A. G. W. (1992). *Jnt CCP4/ESF–EACMB Newsl. Protein Crystallogr.* **26**.

Lovenberg, W., Levine, R. A., Robinson, D. S., Ebert, M., Williams, A. C. & Calne, D. B. (1979). *Science*, **204**, 624–626.

Matthews, B. W. (1968). *J. Mol. Biol.* **33**, 491–497.

Milstien, S., Jaffe, H., Kowlessur, D. & Bonner, T. I. (1996). *J. Biol. Chem.* **271**, 19743–19751.

Nar, H., Huber, R., Meining, W., Schmid, C., Weinkauf, S. & Bacher, A. (1995). *Structure*, **3**, 459–466.

Nichol, C. A., Smith, G. K. & Duch, C. S. (1985). *Annu. Rev. Biochem.* **54**, 729–764.

Otwinowski, Z. & Minor, W. (1997). *Methods Enzymol.* **276**, 307–326.

Rossmann, M. G. & Blow, D. M. (1962). *Acta Cryst.* **15**, 24–31.

Steller, I., Bolotovsky, R. & Rossmann, M. (1997). *J. Appl. Cryst.* **30**, 1036–1040.

Stura, E. A. & Wilson, I. A. (1992). *Crystallization of Nucleic Acids and Proteins, A Practical Approach*, edited by A. Ducruix & R. Giegé, pp. 99–125. Oxford University Press.

Tayeh, M. A. & Marletta, M. A. (1989). *J. Biol. Chem.* **264**, 19654–19658.

Yoneyama, T., Brewer, J. M. & Hatakeyama, K. (1997). *J. Biol. Chem.* **272**, 9690–9696.

Yoneyama, T. & Hatakeyama, K. (1998). *J. Biol. Chem.* **273**, 20102–20108.